The structural phase transition of ZnSe under hydrostatic and nonhydrostatic compressions: an *ab initio* molecular dynamics study

2009 J. Phys.: Condens. Matter 21 125403

(http://iopscience.iop.org/0953-8984/21/12/125403)

J. Phys.: Condens. Matter **21** (2009) 125403 (7pp) doi:10.1088/0953-8984/21/12/125403

The structural phase transition of ZnSe under hydrostatic and nonhydrostatic compressions: an *ab initio* molecular dynamics study

Murat Durandurdu

Department of Physics, University of Texas at El Paso, El Paso, TX, 79968, USA
and
Fizik Bölümü, Ahi Evran Üniversitesi, Kırşehir, 40100, Turkey

Received 23 November 2008, in final form 29 January 2009
Published 26 February 2009
Online at stacks.iop.org/JPhysCM/21/125403

Abstract

Ab initio constant pressure molecular dynamics simulations within a generalized gradient approximation (GGA) are carried out to study the structural phase transformation of ZnSe under hydrostatic and nonhydrostatic conditions. ZnSe undergoes a first-order phase transition from the zinc-blende structure to a rocksalt structure having practically identical transformation mechanisms under hydrostatic and nonhydrostatic compressions. This phase transformation is also analyzed using the enthalpy calculations. Our transition parameters and bulk properties are comparable with experimental and theoretical data. Furthermore, the influence of pressure on the electronic structure of ZnSe is investigated. It is found that the band gap energy increases nonlinearly under both hydrostatic and nonhydrostatic conditions and the effect of stress deviations on the band gap energy is small. The computed pressure coefficients and deformation potential of the band gap are in good agreement with experiments.

(Some figures in this article are in colour only in the electronic version)

1. Introduction

The pressure-induced phase transformations from fourfold-coordinated to sixfold-coordinated structures in binary semiconducting compounds are a fundamental topic in condensed matter physics. Of particular interest are zinc-blende (ZB)-type materials. The ZB to rocksalt (RS) phase transition has been studied extensively for decades and considerable information concerning this phase change has been obtained.

Among ZB-type semiconductors, ZnSe is an important material because of its application in the fabrication of blue lasers. Its behavior under pressure has been a subject of many experimental and theoretical studies [1–10]. With the application of pressure, ZnSe transforms from the ZB structure into a RS structure around 13 GPa [1, 2]. In contrast to these studies, recent Raman experiments [3] reported the existence of anomalies in the equation of state and in the TO and LO Raman frequencies at 5 GPa (the TO and LO modes showed a discontinuity at this pressure). Furthermore, the authors found that ZB phase first transformed to a distorted RS state, specifically a rhombohedral A7 type of structure with $\alpha = 59.4°$ at about 17 GPa, and then an ideal RS state above 47 GPa. Further compression yielded a phase transformation into a simple hexagonal structure near 55 GPa. Lin *et al* [4] also observed similar anomalies around 5.0 and 9 GPa. The author found that the TO phonon splits into two peak components around 5 GPa and it splits into two components again near 9 GPa. The resulting structures at 5 and 9 GPa could not be identified in that experiment but author suggested that ZnSe might undergo a structural phase transformation from the ZB through cinnabar and the orthorhombic (*Cmcm*) to the RS structure at 4.7, 9.1, and 14.4 GPa, respectively, similar to what has been observed for ZnTe. McMahon and Nelmes [5], on the other hand, could not locate any anomalies in these pressure regions. They found a continuous RS to *Cmcm* phase transition near 30.0 GPa and suggested a further distortion above 48.0 GPa. Recently Pellicer-Porres *et al* [6] observed a cinnabar phase within the very small pressure range 10.1–10.9 GPa upon slowly releasing the pressure from

the RS phase. Kusaba and Kikegawa [7] showed that the cinnabar phase forms below 100 °C while the RS crystal directly transforms into the ZB structure above 300 °C.

The theoretical calculations based on density functional calculations predicted the critical pressure for the ZB–RS transition be about 11–15 GPa [8, 9], in good agreement with the experimental observations. The RS crystal was found to be stable up to 36 GPa and above this pressure it becomes unstable against a *Cmcm* distortion [8]. These calculations also predicted the existence of a fourfold-coordinated cinnabar-type phase, intermediate between the ZB and RS phases in a narrow pressure range [9, 10].

These extensive experimental and theoretical studies have significantly improved our understanding of the solid–solid phase transition in ZnSe. Yet the origin of the anomalies reported in [3, 4] is still unknown, but might be related to the sample properties, pressurizing techniques and the degree of the hydrostatic compression.

In this paper, we explore the behavior of ZnSe under hydrostatic and nonhydrostatic pressures using a constant pressure *ab initio* molecular dynamics (MD) technique and characterize the transformation mechanism of the ZB to RS phase transition. Furthermore we investigate the influence of hydrostatic and nonhydrostatic compressions on the electronic properties of ZnSe.

2. Methodology

The calculations were performed with the SIESTA package [11]. The method is based on density functional theory (DFT), adopting a localized linear combination of atomic orbitals basis sets for the description of valence electrons and norm-conserving nonlocal pseudopotentials for the atomic core. The pseudopotential was constructed using the Troullier and Martins scheme [12]. For the exchange–correlation energy we used the generalized gradient approximation of Perdew, Burke and Ernzerhof [13]. The double-ς plus polarized orbitals were employed. The real space grid was equivalent to a plane wave cutoff energy of 150 Ryd. The convergence with respect to the grid cutoff was carefully checked. Above 100 Ryd we found no variation in the energy and the structural parameters. The simulation cell consists of 64 atoms with periodic boundary conditions. We used Γ-point sampling for the Brillouin zone integration. The results were checked with four special **k**-points but this made less than 2.0 meV difference in the energy and no difference in the lattice parameters and the atomic coordinates at zero pressure. The MD simulations were performed using the NPH (constant number of atoms, constant pressure, and constant enthalpy) ensemble. The reason for choosing this ensemble is to remove the thermal fluctuation, which facilitates easier examination of the structure during the phase transformation. Pressure was applied via the method of Parrinello and Rahman [14] and the structure is equilibrated with a period of 1000 time steps (each time step is one femtosecond (fs)) at each applied pressure. We also used the power quenching technique during the MD simulations. In this technique, each velocity component is quenched individually. At each time step, if the force and velocity components have opposite sign, the velocity component is set equal to zero. All atoms or supercell velocities (for cell shape optimizations) are then allowed to accelerate at the next time step. 10 Ryd fs^2 fictitious Parrinello–Rahman mass in the unit of real moment of inertia was found to be suitable for this system.

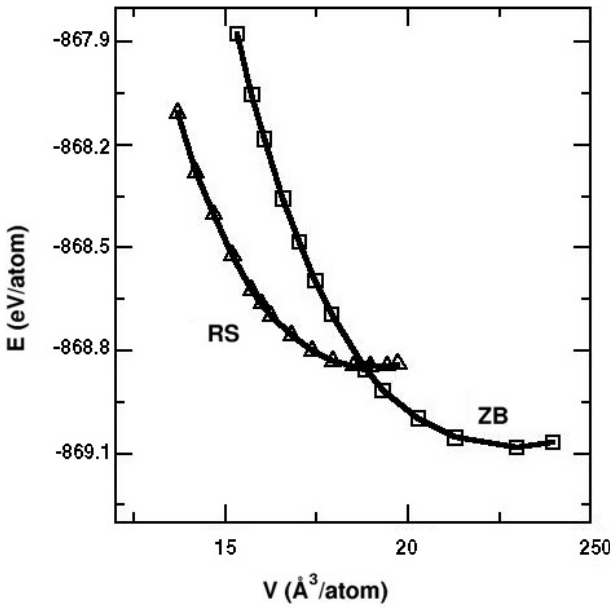

Figure 1. The energy curve as a function of volume for the ZB and RS structured ZnSe.

For the energy–volume calculations, we considered the unit cells for both ZB and RS structures to reduce the computational effort. In order to sample the Brillouin zone, a set of 256 Monkhorst–Pack [15] special **k**-points were used. The both structures were optimized at several volumes and then their enthalpies at zero temperature were calculated.

3. Enthalpy calculations

First we perform calculations to determine the equilibrium parameters of the ZB and RS phases of ZnSe. The unit cell of these structures is relaxed at zero pressure using the variable cell optimization technique. We obtain the lattice constants of the ZB and RS crystals as 5.68 Å and 5.33 Å, respectively. These values are slightly larger than the experimental results of 5.667 Å (for ZB) and 5.299 Å (for RS) [2] and theoretical results of 5.54–5.66 Å for the ZB phase and of 5.17–5.26 Å for the RS phase calculated using local density approximations [8–10] but they are less than 5.82 Å (ZB) and 5.426 Å (RS) computed using a GGA [8].

In the second step, we study the total energy of these structures as a function of volume and fit the energy–volume data to the third-order Birch–Murnaghan equation of state. The computed total energy per atom as a function of volume is shown in figure 1. From the data, we obtain the pressure $P = -\mathrm{d}E_{\mathrm{tot}}/\mathrm{d}V$ and the static enthalpy $H = E_{\mathrm{tot}} + PV$ of the ZB and RS phases. Since at the phase transition, the two phases have the same enthalpy, the transition pressure is determined

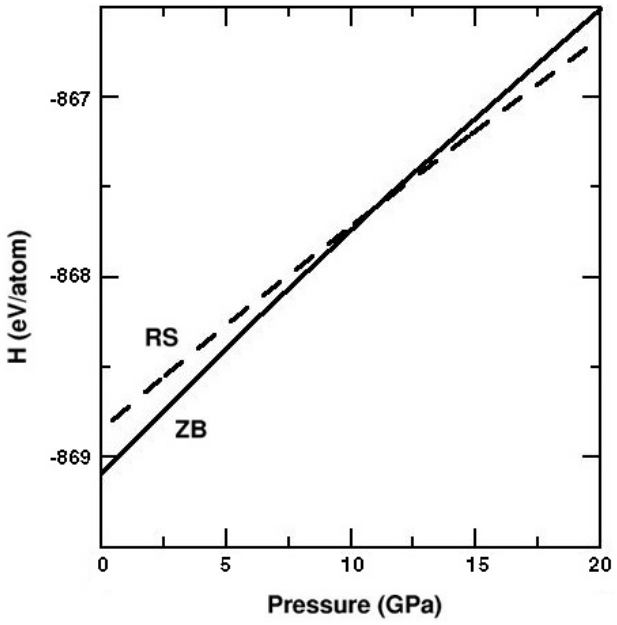

Figure 2. The computed enthalpy curve of the RS and ZB structures. The curves cross around 10.8 GPa, indicating a phase transition from the RS to the ZB structure.

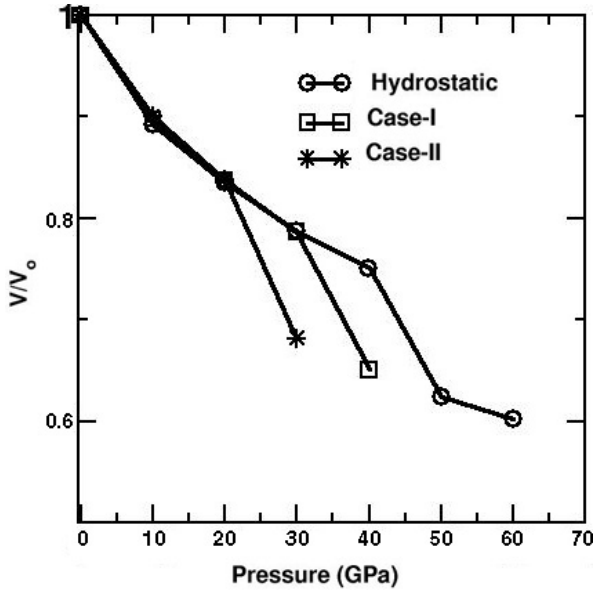

Figure 3. The pressure–volume curve of ZnSe as a function of pressure from the Parrinello–Rahman simulation.

by equating the enthalpies of the two phases. Figure 2 shows the computed enthalpy curve of the ZB and RS states of ZnSe as a function of pressure. As can be seen from the figure, the ZB to RS phase transition occurs at 10.8 GPa, comparable with the experimental value of about 13 GPa [1, 2, 5] and theoretical values of 11–15 GPa [8, 9].

One important property of a material is its bulk modulus (B_0) that can be considered as a fundamental property for determining its stiffness. From the third-order Birch–Murnaghan equation of state, the bulk modulus (B_0) and its pressure derivative (B_0') for the ZB phase are predicted to be 74 GPa and 4.79, respectively. These results agree well with both experimental values of 69.3 GPa [2] and 67 $\pm$ 3 GPa [3] and the theoretical values of 62–81 GPa and 3.81–4.36 [8–10]. For the RS phase, B_0 and B_0' are 98.93 GPa and 3.65, respectively, which are again comparable with 104 GPa (experimental) [2] and 74–92 GPa and 3.47–5.4 (theoretical) [8, 10].

These results demonstrate that the parameters used in the simulation produce satisfactory transition parameters and bulk properties and thus they can be used to explore the pressure-induced phase transition of ZnSe using constant pressure simulations.

4. Dynamical simulation

Figure 3 shows the pressure–volume curve of ZnSe obtained in the dynamical simulation. The volume monotonically decreases up to 50 GPa and at this pressure it shows a significant drop, which is compatible with the first-order phase transition. At 50.0 GPa, ZnSe transforms into a RS state as shown in figure 4. This observation clearly indicates that the *ab initio* technique successfully reproduces the high pressure phase of ZnSe in the dynamical approach as well. Yet, the transition pressure between 40.0 and 50.0 GPa predicted in the simulation is significantly larger than the experimental value of 13.0 GPa. When the particular conditions such as the use of the perfect structure, the size of the simulated structure, timescale of simulations etc are considered, such a tendency is generally expected [16, 17]. This behavior is analogous to superheating in MD simulations. Of course, such a high critical pressure produces transformation parameters that cannot be comparable with those of experiments or enthalpy calculations.

Since an understanding of the transformation procedure is very important to control structural phase transitions, we next analyze the modification of the simulation cell to obtain an atomistic level of understanding of the ZB to RS phase change in ZnSe. The variation of the simulation cell lengths and angles at 50.0 GPa as a function of the MD time step is shown in figure 5. The simulation cell is initially oriented such that its lattice vectors **A**, **B**, and **C** are along the [100], [010] and [001] directions, respectively. The magnitude of these vectors is plotted in the figure. Accordingly, the simulation cell first undergoes a tetragonal distortion with a simultaneous expansion along [100] and [001] directions and a contraction along the [010] direction and then the structure experiences a shear deformation. The β-angle between **A** and **C** changes gradually from 90° to about 110° while other angles remain unchanged up to about 900 MD steps and then slightly deviate from 90°. These small angle deviations result into a slightly distorted RS state. Consequently, the cubic $\rightarrow$ tetragonal $\rightarrow$ monoclinic modification occurs during the phase transformation of ZnSe, similar to that found in SiC using both *ab initio* [18] and classical MD simulations [19], in ZnS [20], and in a model ionic system studied using MD simulations [21].

During the phase transformation, we can easily trace the symmetry change using the KPLOT program. We use 0.2 Å,

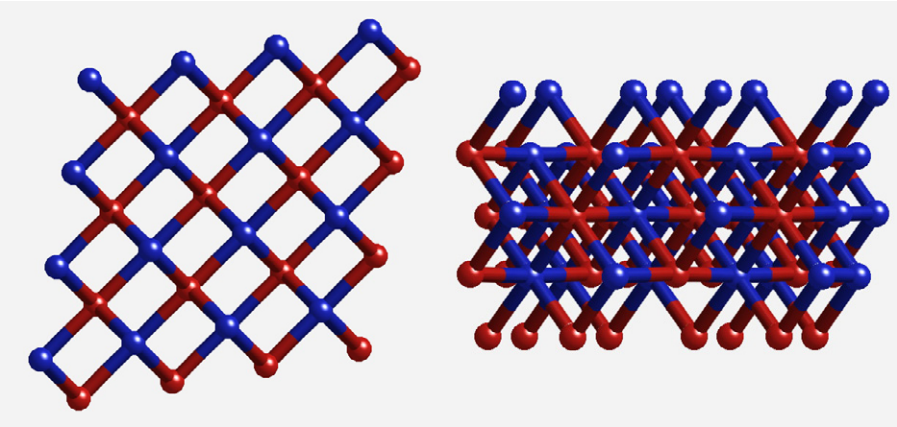

Figure 4. The RS phase formed at 50 GPa in the Parrinello–Rahman simulation. Viewed along (a) [100], (b) [001] directions of the ZB structure.

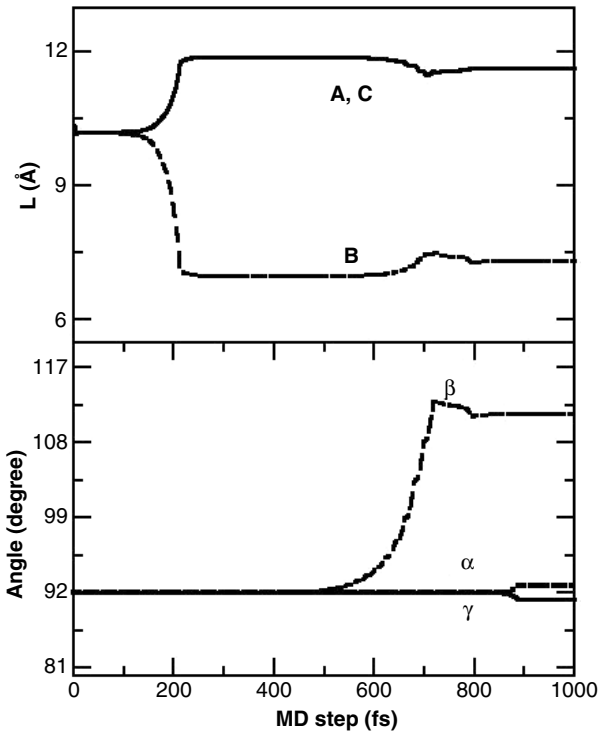

Figure 5. The time evolution of the simulation cell lengths and angles at 50 GPa. The angle between **A** and **B** vectors is α, the angle between **A** and **C** vectors is β, and the angle between **B** and **C** is γ.

4°, and 0.7 Å tolerances for bond lengths, bond angles and interplanar spacing, respectively, for the symmetry analysis. At 153 fs the tetragonal distortion begins and a tetragonal unit cell having space group $I\bar{4}m2$ is formed. Its lattice parameters are $a = b = 4.177$ Å, and $c = 3.537$ Å at 218 fs. This phase is still fourfold coordinated with a bond length of about 2.26 Å and the angles between atoms are 134° and 98°. The tetragonal modification causes the Zn and Se atoms to shift against each other along the compressed direction and the opening and closing the tetragonal angles. With the monoclinic modification of the simulation cell, the angles gradually tend toward 90° and 180°. The opening of the tetrahedron leads to channels for the neighboring atoms to form a sixfold-coordinated structure. The monoclinic modification leads to the formation of an orthorhombic state within $Imm2$ symmetry when the β-angle is about 96°. The unit cell constants of this orthorhombic phase are $a = 4.413$ Å, $b = 3.90$ Å and $c = 3.55$ Å. When the β-angle reaches a value of about 107°, the angles are considerably opened (about 173°) and the neighboring atoms are close enough to form a distorted sixfold-coordinated state in which each atom has four neighbors at a distance of about 2.36 Å and two neighbors at 2.61 Å. At later time steps, almost an ideal RS state with a lattice parameter of 4.87 Å is gradually shaped due to the further relaxation of the structure. The lattice constant of this RS structure, as expected, is considerably smaller than the experimental value of 5.299 Å [2], which is indeed related to the overpressurization of the simulation box.

Although the ZB to RS phase transition is successfully observed in the constant pressure simulation, several factors such as finite size artifacts, overestimated transition pressures, loading conditions (timescale) in the simulations might artificially favor the cubic → tetragonal → monoclinic mechanism.

5. Nonhydrostatic compressions

As pointed out above, experiments [3, 4] reported the existence of anomalies around 5 and 9.0 GPa. These behaviors might be an artifact of nonhydrostatic compressions because the degree of the hydrostaticity in experiments is determined by the efficiency of the pressure-transmitting medium. At high pressures, the pressure-transmitting medium solidifies resulting in strong nonhydrostatic effects. Even in the low pressure regime, pressure in the diamond anvil cell is not exactly hydrostatic. In order to study the influence of the degree of the hydrostatic compression on the phase transformation of ZnSe, we consider two nonhydrostatic conditions and label them as Case I ($\sigma_{xx} = 0.95P, \sigma_{yy} = 0.9P$

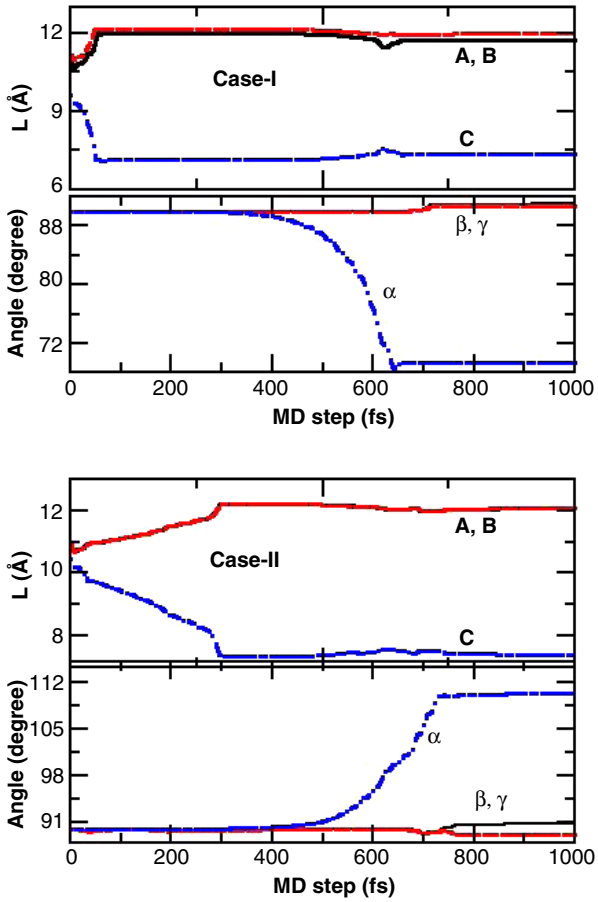

Figure 6. The time evolution of the simulation cell lengths and angles for the nonhydrostatic compressions at the transition pressure of 40 GPa (Case I) and 30 GPa (Case II). The angle between **A** and **B** vectors is α, the angle between **A** and **C** vectors is β, and the angle between **B** and **C** vectors is γ.

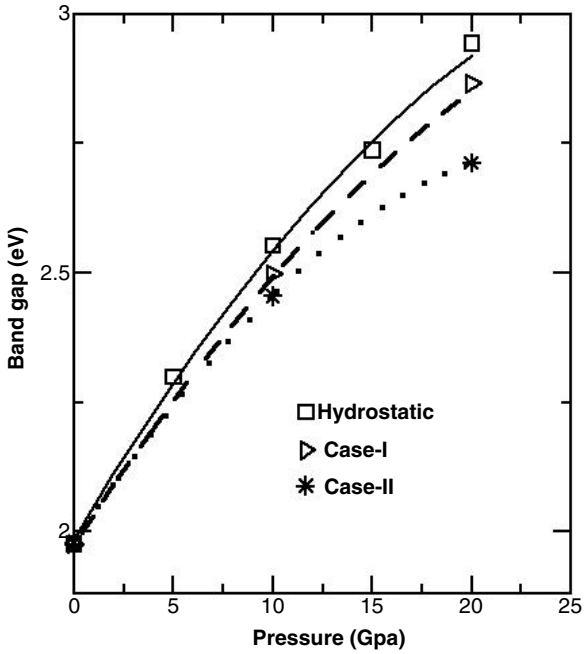

Figure 7. Pressure dependence of the band gap energy.

and $\sigma_{zz} = P$, where P is the applied external pressure and σ_{xx}, σ_{yy} and σ_{zz} are the diagonal components of the stress tensor) and Case II ($\sigma_{xx} = 0.9P$, $\sigma_{yy} = 0.9P$ and $\sigma_{zz} = P$). The volume change under these loading conditions is represented in figure 3. The phase transformation occurs at 40 GPa and 30 GPa for Case I and Case II, respectively. As expected the critical pressure is notably reduced as the stress deviation is increased. For both cases, however, we find no indication of a new phase transformation in ZnSe and instead the ZB structure converts into a RS state. Note that ZnSe transforms into a more open RS state under nonhydrostatic compressions. Furthermore, although the nonhydrostatic compressions break the symmetry of the system before the phase transitions occur, the mechanism obtained in these nonhydrostatic environments (see figure 6) occurs in two stages and is unexpectedly similar to what has been determined in the perfect hydrostatic condition. Therefore, we conclude that the ZB to RS transition pathway of ZnSe is independent of the degree of nonhydrostatic conditions (up to 10% deviations) in the simulations.

These observations suggest that the anomalies reported in [3] and [4] are not associated with the nonhydrostatic compressions but we cannot definitely conclude that this is true because of the limitations mentioned above, in the simulations. These limitations might favor the formation of a RS state even under nonhydrostatic conditions with a similar transformation mechanism. Furthermore, in stark contrast to experimental findings, the simulated structure does not have any defect and such an ideal state might suppress anomalies and produce a similar transformation pathway under both hydrostatic and nonhydrostatic compressions. It might be possible that these anomalies are not associated with the degree of hydrostatic condition alone but with defects or the correlation between defects and nonhydrostatic compressions. Therefore, further studies are desirable, to better understand the roles of the stress deviations, defects, and their correlations on phase transformations.

6. Electronic structure

We finally investigate the influence of the hydrostatic and nonhydrostatic compressions on the electronic structure of ZnSe. The pressure–band gap relations are illustrated in figure 7 in which the lines correspond to a least squares fit of a second-order polynomial. At zero pressure, the GGA band gap is predicted at about 1.98 eV. As expected, this value is smaller than the experimental result, 2.7 eV [22]. It is well known that the DFT-GGA does not accurately describe the band gap energy, which is mainly due to the well-known shortcoming of DFT in describing excited states. However, despite the underestimation of the band gap energy, the variation of bad gaps under pressure is often reproduced reasonably well within the DFT-GGA. With the application of pressure, the band gap energy increases sublinearly, which is in good agreement with experiment [23]. Under pressure, the valence and conduction states near the band gap gradually shift to higher energies but the shift of the conduction states is larger than that of

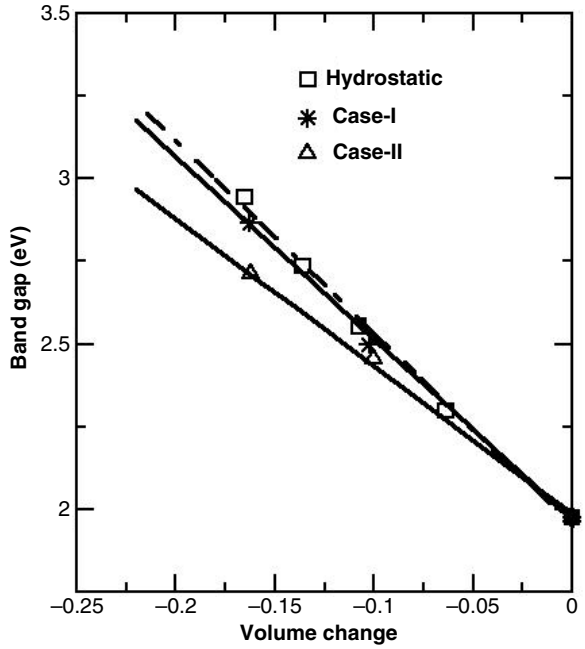

Figure 8. Band gap energy as a function of volume change ($\Delta V/V_0$).

the valence states, yielding such an increase in the band gap. The linear and quadratic pressure coefficients are predicted to be 64 meV GPa^{-1} and -0.9 meV GPa^{-1}, respectively. Our calculated linear pressure coefficient is in excellent agreement with the experimental value of 60–75.7 meV GPa^{-1} [23–25] and the theoretical result of 63 meV GPa^{-1} [26]. We also study the variation of the band gap energy as a function of volume to calculate the deformation potential ($D = \Delta E_{\rm gap}/\Delta V/V_0$, where $\Delta V = V - V_0$ and V_0 is the equilibrium volume at zero pressure). The slope of the best fitting straight line in figure 8 gives an average deformation potential, -5.81 eV. This value also agrees well with the experimental values of -4.8 and -5.40 eV [23, 27] and the theoretical results of -2.69 to -5.82 eV [28–31]. For the nonhydrostatic cases, we again find that the band gap energy increases. The change in the band gap energies is slightly less than that of the hydrostatic pressure. The linear pressure coefficient is calculated to be about 60 m eV GPa^{-1} and 59 m eV GPa^{-1} for Case I and Case II, respectively. The deformation potential is about -5.42 meV for Case I and -4.55 meV for Case II. These results demonstrate that the degree of hydrostatic compression has a small effect on the electronic structure of ZnSe.

7. Conclusions

A constant pressure *ab initio* technique within a GGA is carried out to study the structural phase transitions of ZnSe under hydrostatic and nonhydrostatic compressions. A first-order phase transition from the ZB structure to a RS structure is successfully observed in simulations under these loading conditions. The phase transformations under hydrostatic and nonhydrostatic pressures are associated with the monoclinic modification of the simulation cell and occur in two stages: accompanied by an initial tetragonal distortion and a subsequent shearing, similar to what has been found in other ZB-type materials. From the enthalpy calculations, the ZB to RS phase transition is predicted to occur about 10.8 GPa, in agreement with experiments. Furthermore we observe that the band gap energies increase with the application of hydrostatic and nonhydrostatic pressures. The computed pressure coefficients and deformation potential of the band gap are in good agreement with experiments. Several important conclusions can be stated from the present simulation results for the *defect free* (perfect) ZnSe structure. First, ZnSe transforms into a RS state with the application of hydrostatic nonhydrostatic pressure. Second, the anomalies reported in experiments [3, 4] might not be associated with a hydrostatic effect. Third, the ZB to RS transformation mechanism does not depend on the degree of hydrostatic pressure. Fourth, the effect of stress deviations on the band gap energy is very small. We however do not know the role of crystal defects on structural phase transformations and their transformation mechanism(s) and the correlations between defects and the stress deviations. Therefore, further studies are definitely needed to reveal the origin of anomalies seen experiments.

Acknowledgments

The author is grateful to Dr R Hundt for his valuable help in the use of the KPLOT program and analyzing the structures. The visit of MD to Ahi Evran Üniversitesi was facilitated by the Scientific and Technical Research Council of Turkey (TÜBİTAK) BIDEB-2221. The calculations were run on Sacagawea, a 128-processor Beowulf cluster, at the University of Texas at El Paso.

References

[1] Smith P L and Martin J E 1965 *Phys. Lett.* **19** 541
[2] Karzel H, Potzel W, Köfferlein M, Schiessl W, Steiner M, Hiller U, Kalvius G M, Mitchell D W, Das T P, Blaha P, Schwarz K and Pasternak M P 1996 *Phys. Rev.* B **53** 11 425
[3] Greene R G, Luo H, Ghandehari K and Ruoff A L 1995 *J. Phys. Chem. Solids* **56** 521
[4] Lin C M, Chuu D S, Yang T J, Chou W C, Xu J A and Huang E 1997 *Phys. Rev.* B **55** 13 641
[5] McMahon M I and Nelmes R J 1996 *Phys. Status Solidi* b **198** 389
[6] Pellicer-Porres J, Segura A, Muñoz V, Zúñiga J, Itié J P, Polian A and Munsch P 2001 *Phys. Rev.* B **65** 012109
[7] Kusaba K and Kikegawa T 2002 *J. Phys. Chem. Solids* **63** 651
[8] Smelyansky V I and Tse J S 1995 *Phys. Rev.* B **52** 4658
[9] Côté M, Zakharov O, Rubio A and Cohen M L 1997 *Phys. Rev.* B **55** 13 025
[10] Qteish A and Muñoz A 2000 *J. Phys.: Condens. Matter* **12** 1705
Hamdi I, Aouissi M, Qteish A and Meskini N 2006 *Phys. Rev.* B **73** 174114 and references therein
[11] Ordejón P, Artacho E and Soler J M 1996 *Phys. Rev.* B **53** 10441
Sánchez-Portal D, Ordejón P, Artacho E and Soler J M 1997 *Int. J. Quantum Chem.* **65** 453
[12] Troullier N and Martins J L 1997 *Phys. Rev.* B **43** 1993
[13] Perdew J P, Burke K and Ernzerhof M 1996 *Phys. Rev. Lett.* **77** 3865

[14] Parrinello M and Rahman A 1980 *Phys. Rev. Lett.* **45** 1196
[15] Monkhorst H J and Pack J D 1976 *Phys. Rev.* B **13** 5188
[16] Martoñák R, Laio A and Parrinello M 2003 *Phys. Rev. Lett.* **90** 75503
[17] Mizushima K, Yip S and Kaxiras E 1994 *Phys. Rev.* B **50** 14952
[18] Durandurdu M 2004 *J. Phys.: Condens. Matter* **16** 4411
[19] Shimojo F, Ebbsjö I, Kalia R, Nakano A, Rino J P and Vashista P 2000 *Phys. Rev. Lett.* **84** 3338
[20] Martinez I and Durandurdu M 2006 *J. Phys.: Condens. Matter* **18** 9483
[21] Wilson M, Hutchinson F and Madden P A 2002 *Phys. Rev.* B **65** 94109
[22] Ley L, Pollak R A, McFeely F M, Kowalczyk S P and Shirley D A 1974 *Phys. Rev.* B **9** 600
[23] Ves S, Strössner K, Christensen N E, Kim C K and Cardona M 1985 *Solid State Commun.* **56** 479
[24] Jaszczyn-Kopec A, Canny B and Syfosse C 1983 *J. Lumin.* **28** 319
[25] Cardona M 1963 *J. Phys. Chem. Solids* **24** 1543
[26] Gorczyca I and Christensen N E 1993 *Phys. Rev.* B **48** 17202
[27] Madelung O, Schulz M and Weiss L 1982 *Physics of II–VI and I–VII Compounds, Semimagnetic Semiconductors* (*Landolt–Börnstein New Series, Group III* vol 17, Pt b) (Berlin: Springer) and references therein
[28] Shahzad K, Olego D J and Van de Walle C G 1988 *Phys. Rev.* B **38** 1417
[29] Qteish A, Said R, Meskini N and Nazzal A 1995 *Phys. Rev.* B **52** 1830
[30] Bernard J E and Zunger A 1987 *Phys. Rev.* B **36** 3199
[31] Cardona M and Christensen N E 1987 *Phys. Rev.* B **35** 6182